Research Article Vol. 61, No. 16 / 1 June 2022 / Applied Optics 4927

applied optics

Silicon photonics 2 × 2 trench coupler design and foundry fabrication

Hiva Shahoei,[1] Ifeanyi G. Achu,[1] Evan J. Stewart,[1] Unaiza Tariq,[1] William V. Oxford,[2] Mitchell A. Thornton,[1] and Duncan L. MacFarlane[1,*]

[1]Southern Methodist University, Dallas, Texas 75275, USA
[2]Anametric, Inc, Austin, Texas 78759, USA
*Corresponding author: dmacfarlane@smu.edu

Received 12 January 2022; revised 10 May 2022; accepted 10 May 2022; posted 13 May 2022; published 27 May 2022

A 2 × 2 photonic coupler is realized at the intersection of two 480 nm × 220 nm silicon on insulator waveguides. The designed 2 × 2 coupler is simulated in both High Frequency Simulator System (HFSS) and Lumerical and shows an equal split of an input signal into transmitted and reflected signals for a 45 deg, ∼100 nm SiO_2 filled trench. The principle of operation of the coupler is frustrated total internal reflection. Thus, this behavior is reasonably flat across wavelength, which is confirmed by Lumerical simulations and by experiment. Also, it has been shown that this coupler has a flat behavior across trench thickness for the chosen geometry and material system, which makes it insensitive to fabrication variation and resolution. We are interested to make this coupler a part of silicon photonic foundry process development kits. Therefore, fabrication is done at the AIM Photonics Foundry to study the performance in the context of the foundry's design rules and process flow of the foundry. Good agreement between theory and experiment is reported herein. A 2 × 2 trench coupler is, when operated in the single photon or quantum regime, an integrated photonic realization of a Hadamard gate.

https://doi.org/10.1364/AO.453464

1. INTRODUCTION

Sub-micrometer etched beam splitters have been studied by several groups of researchers [1–12]. Compact 1 × 2 90 deg splitters in silicon on insulator (SOI) rib waveguides were designed and tested [1–3]. Similar 1 × 2 90 deg splitters in III-V materials have been realized [2,5–7,9,10], where challenges due to the demand for high aspect ratio etching were encountered [11,12]. In addition to a 1 × 2 splitter, a four-port nanophotonic coupler was realized in InP [7]. A 1 × 2 trench-based photonic coupler was also realized in ion-exchange glassware [8].

Applications of interest for submicrometer etched beam splitters include, to date, splitter networks, ring lasers, coherent receivers, passive, active, and programmable filters, and Mach–Zhender switches and modulators [3,13–17]. In addition, quantum photonic integrated circuits (PICs) would benefit from the 2 × 2 integrated photonic coupler reported herein. Beam splitters are widely used as Hadamard gates in tabletop quantum optical experiments [18–20]. These splitters work based on frustrated total internal reflection (FTIR), and a 2 × 2 trench coupler is the exact miniaturization of it.

Photonic integration today is being accelerated by the foundry model wherein the high fixed cost assembling and operating of a nanofabrication facility are, through standardization, amortized across a large number of small to moderate markets. It is the interest of this research team to develop trench couplers consistent with the process development kits (PDKs) of silicon photonic foundries. Therefore, the coupler is foundry fabricated to study the performance in the context of the foundry fabrication process. To the best of our knowledge, herein we present the very first SOI 2 × 2 trench coupler fabricated in a multi-project wafer (MPW) foundry run, which is a path for widespread adoption. The 2 × 2 trench coupler test structures were included on a PIC fabricated on 300 mm wafers using the 65 nm process in place for the AIM Photonics MPW service [21].

2. THEORY OF OPERATION

In Fig. 1 is shown a scanning electron micrograph showing a top view of one of the fabricated trench couplers. In the sample preparation, the SiO_2 dielectric fill in the trench was etched away. From this figure, the operation of the integrated photonic component can be, mostly, intuited. Light propagating in any one input branch is divided into reflected and transmitted components upon two output branches.

In semiconductor-based integrated photonic systems, the index of the waveguides, Si, SiN, or InP, for example, is sufficiently higher than air or a dielectric fill so that, for most values

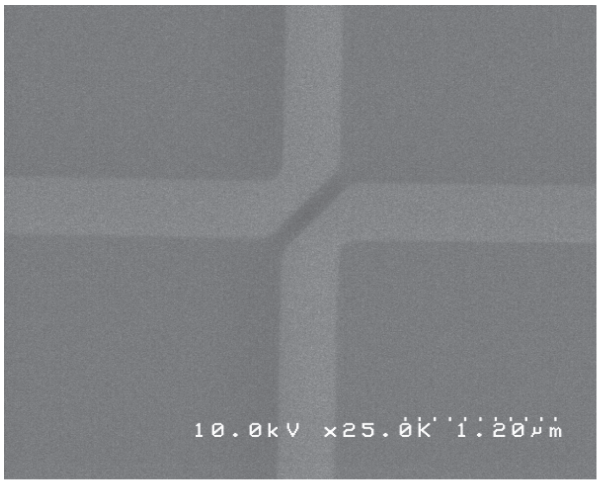

Fig. 1. SEM of a fabricated trench coupler. The design specification of the width of this particular trench was 105 nm. The SiO_2 coating and trench fill were etched away during sample preparation.

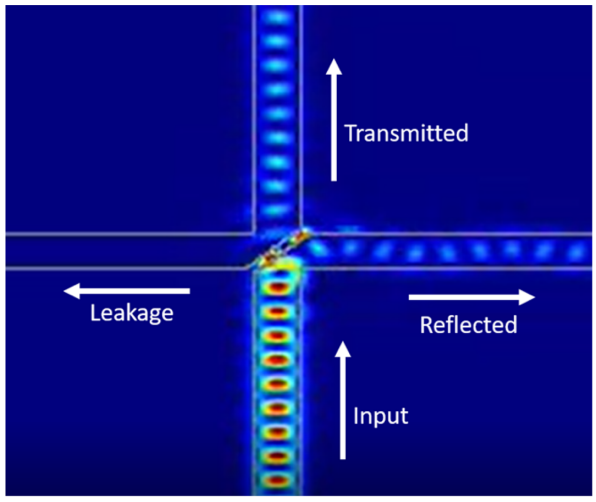

Fig. 2. FDTD calculation of the propagating E-field in a 104 nm wide trench coupler, using Lumerical FDTD software.

of the eikonals or k-vectors of a mode, the interaction of a 45 deg semiconductor–dielectric interface is total internal reflection (TIR). If the trench is sufficiently narrow, this TIR is frustrated so that the field is not fully reflected; a portion evanescently couples to the waveguide beyond the trench. Thus, the analytic theory of a 1×2 trench coupler developed by Huntoon *et al.* [4] is based on FTIR, wherein a portion of the mode incident on the trench evanescently couples to the continuing waveguide, while a second portion is reflected into the orthogonal waveguide. This analytic theory neglects the curvature of the mode in both directions across its face, and hence, in practice, a small additional portion of the incident mode is lost. In this 1×2 mode of operation, maximum efficiency is obtained by offsetting the location of the trench to account for the Goos–Hanchen phase shift. Symmetry demands for a 2×2 coupler are a compromise to this constraint [4].

3. DESIGN OF THE TEST STRUCTURE

The precise design in this work was performed using commercial finite difference time domain (FDTD) software packages. Both Lumerical and High Frequency Simulator System (HFSS) were used with excellent agreement to model the operation of the trench couplers realized by a 45 deg, SiO_2 filled trench at the intersection of two 480 nm × 220 nm SOI waveguides. The trench in Fig. 2 was simulated in Lumerical FDTD 2020a. A source with wavelength 1.55 µm was used. The simulation shows equal splitting of an input signal into transmitted and reflected signals at ∼100 nm trench width (Fig. 5). Given that the fundamental principle is FTIR, there is no interreference phenomenon in the operation of this device; therefore, wavelength independency is expected for this coupler.

In Fig. 3 is shown the arrangement of the trench coupler test structures. The layout editor software package L-Edit [22] was used for chip layout and to generate the GDSII file submitted to AIM Photonics. Input and output access to the trench couplers was accomplished using grating couplers, standard to the AIM Process Development Kit (AIM PDK 3.5a), spaced at a 127 µm pitch to match a fiber array. The silicon waveguides were 480 × 220 nm structures. To define the trench in L-Edit, a cut of the amount corresponding to the trench width was made into the corner of each of the four intersecting 480 nm wide waveguides, and a triangular section of Si was then added to fit into the two waveguide sections. Upon processing, this trench was etched and then backfilled with SiO_2. Waveguide loopbacks (U-turns) were included around the trench coupler test structures to aid in alignment and also to normalize the output powers measured in each branch of a coupler under test.

4. CHARACTERIZATION

A. Physical Characterization

A representative die was etched and imaged in a scanning electron microscope (SEM). Any SiO_2 fill in the trench was sacrificed in the etch process of the sample preparation. The SEM allowed measured estimates of the yielded trench widths. Fig. 1, previously discussed, is an example of a successfully realized 2×2 trench coupler. In this case, the designed trench width was 105 nm, and the measured trench width was 141 ± 6 nm. Not all designed trench widths yielded; those with dimensions 80 nm or smaller were not realized. Further, all the trenches that did yield (85, 95, 105, 115, and 125 nm) produced trenches that were measured to be ∼30% wider than specified. These data are summarized in Fig. 3.

B. Functional Characterization

The block diagram of the measurement setup is shown in Fig. 4. A 1550 nm diode laser was directly modulated at 1 KHz. The input signal from the laser passes through a polarization controller and into the desired fiber of the fiber array. Mechanical alignment between the fiber and the PIC was achieved with an angled fiber array mounted on a six-axis translation stage. Three inspection microscopes were deployed to provide feedback for the coupling alignment. In addition, a visible (red) laser coupled into two of the fibers of the array provided alignment beacons to position the array over the grating couplers of the desired test structure. After traveling through the trench coupler under test

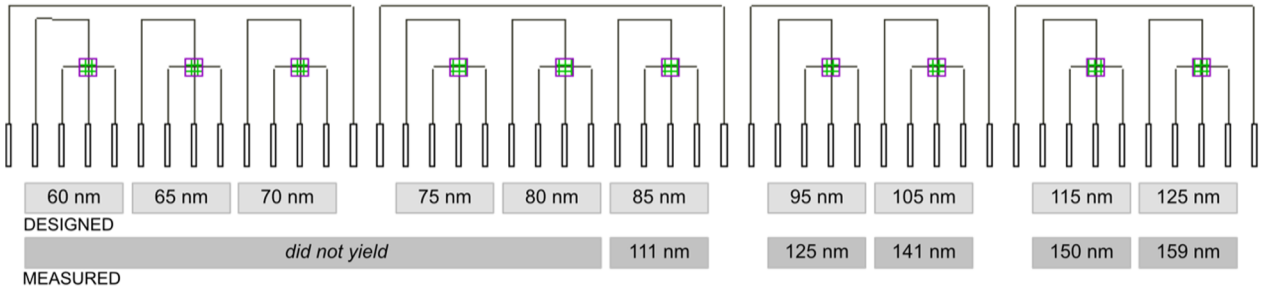

Fig. 3. Mask design of the 2 × 2 trench coupler test structures including the range of designed and, where realized, measured trench widths. The standard deviation error on the measured trench widths is ∼6 nm. The trench couplers were accessed through grating couplers. Waveguide loopbacks (U-turns) are included around the test structures to aid in alignment and to normalize the output powers measured in each branch.

on the PIC, the signal exits through a vertical grating coupler, back into the fiber array, and onto a photodetector. Lock-in detection at 1 kHz modulation increased the dynamic range of the measurement, and this was necessary to resolve the splitting ratios and overall efficiencies.

On the PIC, the trenches of various thicknesses are grouped by a surrounding U-turn structure. This U-turn is used not only for the purpose of alignment but also for normalization of the measured power during coupler characterization. The fiber array is first aligned such that the signal through the U-turn is maximized by adjusting the x and y axes and the transfer function of the polarization controller. The maximum signal strength through the U-turn structure is used when normalizing the results from each trench within the group. The laser signal is sent to a fiber corresponding to the input of a trench, and the transmission, reflection, and leakage into the lee side of the trench are measured. The above process is then repeated for a different orientation of the trench (the waveguides corresponding to input, reflection, transmission, and leakage are rotated). Once each trench in the group has been tested, the U-turn signal is measured again to ensure a consistent alignment through the measurements. At least three full sets of data were collected for each trench thickness. Also, we used the U-turn measurements for normalization and thus for estimating coupler efficiency. Normalized power (measured, and calculated by FDTD) is plotted in Fig. 5 as a function of measured trench width for the yielded couplers for two different dies. The dotted lines in both cases are calculated by FDTD. Superimposed on these theoretical lines are the measured values for the realized trenches.

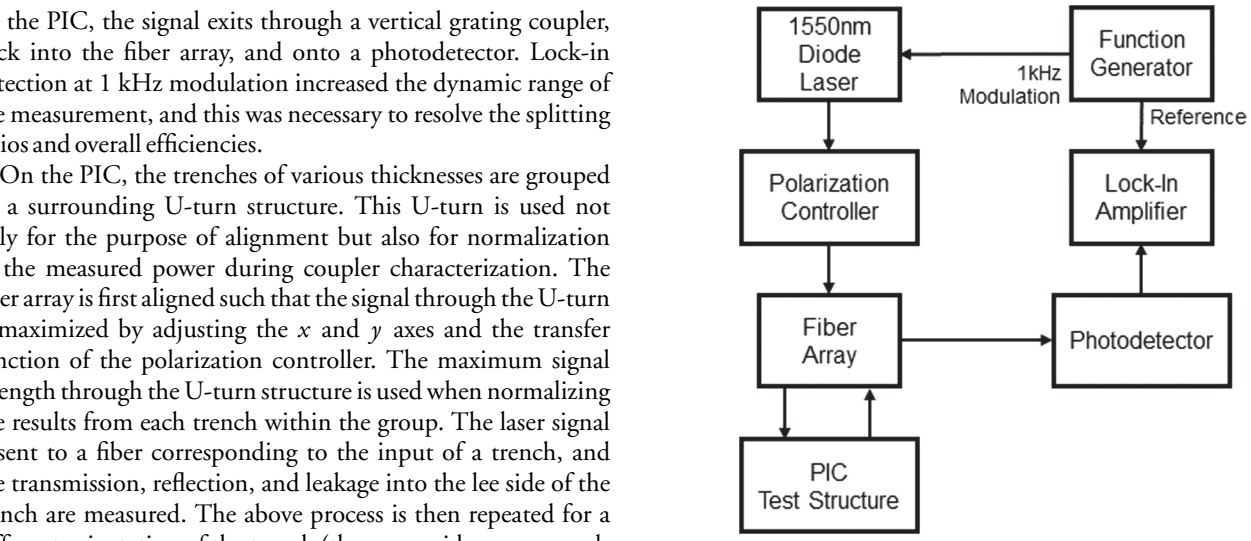

Fig. 4. Block diagram of the integrated trench coupler measurement setup.

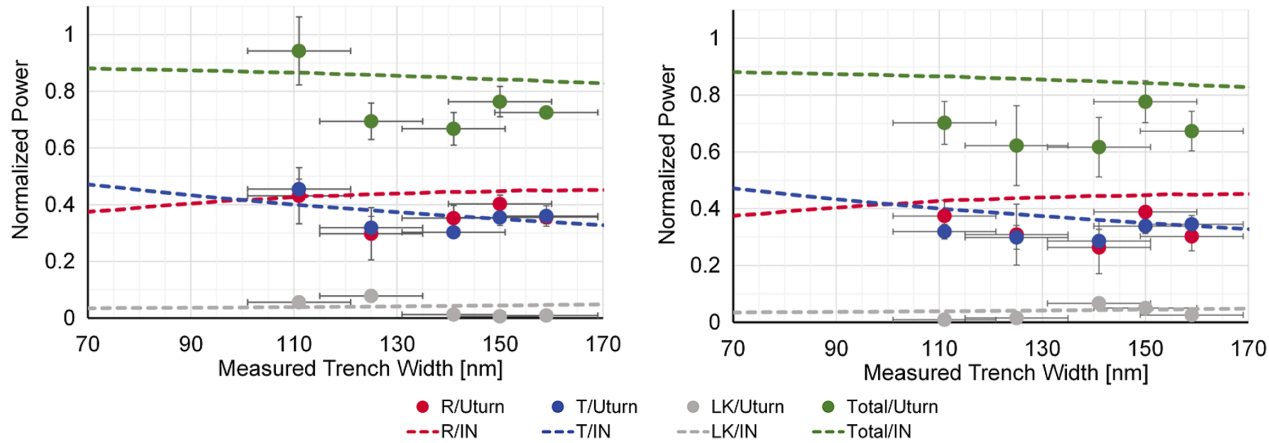

Fig. 5. Normalized port powers for realized trenches. The dotted lines in both cases are calculated by FDTD. Superimposed on these theoretical lines are the measured values. R/Uturn, T/Uturn, LK/Uturn, and Total/Uturn are measured reflection, transmission, leakage, and their summation, respectively, which are normalized to the U-turn power. R/IN, T/IN, LK/IN, and Total/IN are simulated reflection, transmission, leakage, and their summation, respectively, which are normalized to the input power.

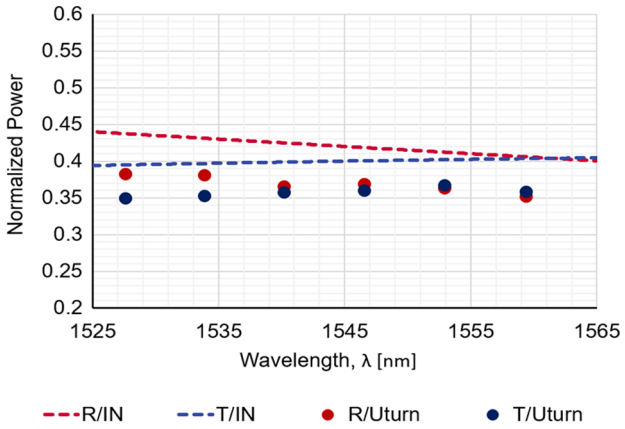

Fig. 6. Normalized port powers for a 100 nm wide trench coupler across C-band (1525–1565 nm). The dotted lines are calculated by FDTD. Superimposed on these theoretical lines are the measured values. R/IN and T/IN are simulated reflection and transmission, respectively, which are normalized to the input power. R/Uturn and T/Uturn are measured reflection and transmission, respectively, which are normalized to the U-turn power.

The calculated reflection, transmission, and leakage coefficients correspond to the magnitude of the S parameters. Balanced coupling (equal reflection and transmission) is predicted theoretically at ∼100 nm, but no trenches of that size yielded. Measured reflection coefficients, transmission coefficients, and leakage are in reasonable agreement with the Lumerical FDTD calculations. The measured efficiency is lower than calculated, and hence, there is a ∼1.2 dB total loss that includes the 5% (0.22 dB) leakage from the coupler.

The wavelength dependency of this coupler is also studied theoretically and experimentally. Figure 6 shows the transmission and reflection of a 100 nm trench coupler in the C-band (1525–1565 nm). As can be seen, a flat behavior is observed in the C-band. The dotted lines are calculated by FDTD. Superimposed on these theoretical lines are the measured values. The simulation and theory both show less than 5% deviation from a 50/50 splitting ratio in the C-band for this trench coupler.

5. CONCLUSION

In this work, we have designed and tested 2 × 2 trench couplers fabricated at the AIM Photonics Foundry. The principle of operation of the coupler is FTIR. This behavior is reasonably flat across wavelength and for our chosen geometry and material system, surprisingly flat across trench thickness. We have used a U-turn structure for characterization of the trench couplers and efficiency estimation. The inherent loss of the component is calculated to be −0.6 dB, which is similar to conventional Y-couplers. Part of this inherent loss is due to the symmetry demanded by a 2 × 2 configuration. The excess loss of the realized structure was measured to be an additional −0.6 dB. A post-etch dielectric fill of the coupling trench is consistent with the fabrication process, and the increased index of refraction of SiO_2 enables a wider trench (∼100 nm) for equal splitting. In this system, an air gap of ∼34 nm would provide a similar equal splitting. This narrow air gap trench would also provide for a lower inherent loss (−0.4 dB) because more of the mode's k-vectors match the TIR condition.

Several groups of authors have described this structure as "compact" or "ultra-compact" [1–3,8–10,14,16,17]. From Fig. 2, we know that some additional waveguide distance is needed to settle the mode. Taking this into account, the area reduction of the trench coupler over conventional Y-junction couplers is approximately 25-fold. As PICs grow in complexity, the value of this reduction in die real estate usage will increase.

It is an interest of this research team to develop quantum PICs. This 2 × 2 trench coupler is, when operated in the single photon or quantum realm, an integrated photonic realization of a Hadamard gate. The symmetry of a 2 × 2 photonic coupler is slightly suboptimal, because in a 1 × 2 waveguide splitter, the design can take into account the Goos–Hanchen phase shift [4], and work is underway to lower both the realization loss and inherent loss to support multi-gate single photon applications.

Funding. U.S. Air Force (FA8649-20-9-9103).

Acknowledgment. The authors thank Dr. Michael L. Fanto, USAF/AFRL, for his continuing advice and knowledgeable support of this project, and Muralidhar Madabhushi Balaji for his help in the early stages of the characterization work. SEM images from Priority Labs, Richardson, TX.

Disclosures. The authors declare no conflicts of interest.

Data availability. Data underlying the results presented in this paper are not publicly available at this time but may be obtained from the authors upon reasonable request.

REFERENCES

1. S. Kim, G. P. Nordin, J. Cai, and J. Jiang, "Ultracompact high-efficiency polarizing beam splitter with a hybrid photonic crystal and conventional waveguide structure," Opt. Lett. **28**, 2384–2386 (2003).
2. Y. Qian, J. Song, S. Kim, and G. P. Nordin, "Compact 90° trench-based splitter for silicon-on-insulator rib waveguides," Opt. Express **15**, 16712–16718 (2007).
3. Y. Qian, J. Song, S. Kim, W. Hu, and G. P. Nordin, "Compact waveguide splitter networks," Opt. Express **16**, 4981–4990 (2008).
4. N. R. Huntoon, M. P. Christensen, D. L. MacFarlane, G. A. Evans, and C. S. Yeh, "Integrated photonic coupler based on frustrated total internal reflection," Appl. Opt. **47**, 5682–5690 (2008).
5. B. Kim and N. Dagli, "Submicron etched beam splitters based on total internal reflection in GaAs-AlGaAs waveguides," J. Lightwave Technol. **28**, 1938–1943 (2010).
6. E. J. Norberg, J. S. Parker, S. C. Nicholes, B. Kim, U. Krishnamachari, and L. A. Coldren, "Etched beam splitters in InP/InGaAsP," Opt. Express **19**, 717–726 (2011).
7. D. L. MacFarlane, M. P. Christensen, K. Liu, T. P. LaFave, G. A. Evans, N. Sultana, T. W. Kim, J. Kim, J. B. Kirk, N. Huntoon, A. J. Stark, M. Dabkowski, L. R. Hunt, and V. Ramakrishna, "Four-port nanophotonic frustrated total internal reflection coupler," IEEE Photon. Technol. Lett. **24**, 58–60 (2012).
8. K. Liu, H. Huang, S. X. Mu, H. Lin, and D. L. MacFarlane, "Ultra-compact three-port trench-based photonic couplers in ion-exchanged glass waveguides," Opt. Commun. **309**, 307–312 (2013).
9. C. Zhang, B. Guan, B. Qi, and K. Liu, "Highly efficient and ultracompact InP/InGaAsP three-port trench-based couplers," Appl. Opt. **59**, 825–832 (2020).
10. N. Rahmanian, S. Kim, Y. Lin, and G. P. Nordin, "Air-trench splitters for ultra-compact ring resonators in low refractive index contrast waveguides," Opt. Express **16**, 456–465 (2008).
11. W. Zhou, N. Sultana, and D. L. MacFarlane, "HBr-based inductively coupled plasma etching of high aspect ratio nanoscale trenches in GaInAsPInP," J. Vac. Sci. Technol. **26**, 1896–1902 (2008).

12. N. Sultana, W. Zhou, T. P. Lafave, Jr., and D. L. MacFarlane, "HBr based inductively coupled plasma etching of high aspect ratio nanoscale trenches in InP: considerations for photonic applications," J. Vac. Sci. Technol. **27**, 2351–2356 (2009).
13. J. S. Parker, E. J. Norberg, Y.-J. Hung, B. Kim, R. S. Guzzon, and L. A. Coldren, "InP/InGaAsP flattened ring lasers with low-loss etched beam splitters," IEEE Photon. Technol. Lett. **23**, 573–575 (2011).
14. U. Krishnamachari, S. Ristic, C. H. Chen, L. Johansson, A. Ramaswamy, J. Klamkin, E. Norberg, J. E. Bowers, and L. A. Coldren, "InP/InGaAsP-based integrated 3-dB trench couplers for ultra-compact coherent receivers," IEEE Photon. Technol. Lett. **23**, 311–313 (2011).
15. D. L. MacFarlane, M. P. Christensen, A. E. Nagdi, G. A. Evans, L. R. Hunt, N. Huntoon, J. Kim, T. W. Kim, J. Kirk, T. P. LaFave, K. Liu, V. Ramakrishna, M. Dabkowski, and N. Sultana, "Experiment and theory of an active optical filter," IEEE J. Quantum Electron. **48**, 307–317 (2012).
16. S. Wang, L. Wang, L. Zhao, B. Qi, and K. Liu, "Compact InGaAsP/InP asymmetric Mach-Zehnder coupled square ring modulator," IEEE Photon. Technol. Lett. **29**, 1312–1315 (2017).
17. K. Liu, L. Wang, C. Zhang, Q. Ma, and B. Qi, "Compact InGaAsP/InP nonblocking 4×4 trench-coupler-based Mach–Zehnder photonic switch fabric," Appl. Opt. **57**, 3838–3846 (2018).
18. U. Leonhardt, *Measuring the Quantum State of Light* (Cambridge University, 1997).
19. J. J. Thorn, M. S. Neel, V. W. Donato, G. S. Bergreen, R. E. Davies, and M. Beck, "Observing the quantum behavior of light in an undergraduate laboratory," Am. J. Phys. **72**, 1210–1219 (2004).
20. M. Beck, "Comparing measurements of $g^{(2)}$ (0) performed with difference detection techniques," J. Opt. Soc. Am. B **24**, 2972–2978 (2007).
21. "American Institute for Manufacturing (AIM) Photonics: multi-project wafer service," http://www.aimphotonics.com/mpw.
22. https://eda.sw.siemens.com/en-US/ic/ic-custom/photonic/l-edit-photonics.